

A new reference block for field gamma spectrometry applications in ESR and luminescence dating

Mathieu Duval^{1,2,3*}, Miren del Val¹, María Jesús Alonso Escarza¹, Lee J. Arnold⁴,
Martina Demuro⁴, Verónica Guilarte⁵, Raju Kumar⁶, Norbert Mercier⁷, Jean-Luc Schwenninger⁶,
Chantal Tribolo⁷, Gloria I. López^{1,8,9,10}

¹ Centro Nacional de Investigación Sobre Evolución Humana (CENIEH),
Paseo Sierra de Atapuerca 3, 09002 Burgos, Spain

² Australian Research Centre for Human Evolution (ARCHE), Griffith University, Nathan QLD 4111, Australia

³ Palaeoscience Labs, Dept. Archaeology and History, La Trobe University, Melbourne Campus, Bundoora, Victoria, Australia

⁴ School of Physics, Chemistry and Earth Sciences, Environment Institute, and Institute for Photonics and Advanced Sensing (IPAS), University of Adelaide, North Terrace Campus, Adelaide, SA, 5005, Australia

⁵ Departamento de Didáctica de las Ciencias Experimentales. Facultad de Ciencias de la Educación y del Deporte de Melilla, Universidad de Granada. Santander 1, 52005, Melilla, Spain

⁶ Research Laboratory for Archaeology and the History of Art, School of Archaeology,
University of Oxford, Oxford OX1 3TG, UK

⁷ Archéosciences Bordeaux, CNRS-University of Bordeaux Montaigne, Maison de l'Archéologie,
Esplanade des Antilles, 33607, Pessac, France

⁸ Colombian Geological Society, Carrera 32A # 25B-83, Torre 5, Local 105, Bogotá D.C., 111321, Colombia

⁹ Nuclear Affairs Directorate, Colombian Geological Survey, Sede CAN,
Carrera 50 # 26-20, Bogotá D.C., 111321, Colombia

¹⁰ Leon Recanati Institute for Maritime Studies (RIMS), University of Haifa, 99 Aba Khoushy Ave,
Mt Carmel, Haifa, 3498838, Israel

*Corresponding Author: mathieu.duval@cenieh.es

Received: October 15, 2024; in final form: December 13, 2024

Abstract

A new granite-doped concrete block with 60 cm × 60 cm × 60 cm dimensions has been built at CENIEH, Burgos, Spain, for dosimetry calibration and cross-referencing purposes. Independent evaluations of the block's gamma dose rate using passive Al₂O₃:C dosimeters and various field gamma spectrometer (NaI) probes produce consistent results of 1495 ± 51 μGy a⁻¹ and 1514 ± 43 μGy a⁻¹ (or 1537 ± 19 μGy a⁻¹, depending on the evaluation procedure employed), respectively. Bulk radioelement concentrations calculated from field gamma spectrometry using the Windows

method are as follows: K = 1.58 ± 0.08 %, U = 4.26 ± 0.28 ppm, and Th = 12.62 ± 0.72 ppm. This new block complements existing dosimetry reference materials accessible at other laboratories and is available for the broader trapped charge dating community to use for instrument calibration, reproducibility assessments and intercomparison studies.

Keywords: Granite-doped concrete block, Calibration, In-situ dosimetry, Field gamma spectrometry, Scintillation detectors, NaI probe, ESR dating, Luminescence dating

1. Introduction

The in situ evaluation of natural radioactivity is a crucial component of trapped charge dating methods such as Electron Spin Resonance (ESR) and Luminescence (including Optically Stimulated Luminescence [OSL], Infrared and Post-Infrared Infrared Stimulated Luminescence [IRSL, pIR-IRSL], Infrared Radiofluorescence [IR-RF] and Thermoluminescence [TL]). This is particularly important in heterogeneous sedimentary environments where it can be difficult to reliably evaluate spatially averaged gamma dose rates from laboratory analyses of discrete sediment samples alone. Passive dosimeters (e.g., OSL or TL dosimeters) or portable gamma-ray spectrometers (mostly NaI or LaBr probes) are usually employed for this purpose. The calibration of the latter is typically performed using reference blocks (e.g., Rhodes & Schwenninger, 2007; Martin, 2015), pads (e.g., Grasty & Minty, 1990), or rocks (e.g., Miallier et al., 2009) of known radioelement concentrations or gamma dose rates. While the Oxford blocks are arguably the most widely used, or at least historically significant, within the community (Bowman, 1976; Murray et al., 1978; Murray, 1981; Stokes, 1994; Rhodes & Schwenninger, 2007; Mercier & Falguères, 2007; Arnold et al., 2012; Duval & Arnold, 2013), other suitable reference blocks exist at various luminescence dating laboratories, including the Scottish Universities Environmental Research Centre (SUERC, UK) Martin (2015), the University of Bordeaux (France) (Richter et al., 2010), the University of Clermont Auvergne (France) (Miallier et al., 2009), and the Geological Survey of Israel (Porat & Halicz, 1996), amongst others. To complement these existing reference materials, the construction of a new granite-doped concrete block was initiated by one of our team members (G. I. L.) in October 2019 at the National Research Centre on Human Evolution (CENIEH) in Burgos, Spain, for dosimetric calibration purposes. Here, we provide some basic information about this new reference block, including the results of various characterisation measurements made using different methods and intercomparison studies undertaken by different research groups.



Figure 1: Picture of the Porriño granite, before (A) and after (B) crushing.

2. The CENIEH reference block

In 2018, the pavement of Burgos city's main square (the Plaza Mayor) was changed to granite slabs extracted from the quarries of Porriño, Pontevedra, Spain. Commercially known as 'Rosa Porriño' (Fig. 1), this coarse-grained, phaneritic and polychromatic biotite granite, especially popular for its pinkish tone, has been widely used both nationally and internationally as an ornamental stone. It is mostly composed of quartz, potassium feldspars, plagioclase and biotite, while accessory minerals include chlorite, epidote and sericite (see detailed description in Grossi et al., 2007). The age of the granite has been constrained by U-Pb dating of selected zircons, providing an age range of 290–295 Ma, i.e., consistent with previous estimates (see Gonzalez Menéndez et al., 2017, and references therein).

In June and October 2018, the Municipality of Burgos (through the company Construcciones Ortega S.A.) donated G. I. L. a total of ten slabs of Pink Porriño granite weighing about 350 kg, which were initially sliced and then crushed to sand/gravel size (Figs. 1, A1 and A2). The construction of the block was performed on-site on 22 October 2019 using a 65 cm × 65 cm × 65 cm wooden formwork, internally coated with 5 cm-thick styrofoam slabs, and positioned onto a wooden pallet to avoid contact with the ground (Fig. A3). Cement (~125 kg), clean (washed) sand aggregate (~100 kg), crushed Porriño granite (~350 kg) and water were mixed using a clean concrete mixer. Given the limited size of the latter, two mixtures (A and B, see Fig. A4) using the same proportion of each component were prepared and the formwork was filled in four successive phases. The mixture was carefully poured into the formwork by hand, using a shovel, avoiding splashes, smearing the mixture with a trowel, avoiding bubbles and cavities. No vibration was applied. In order to evaluate the gamma dose rate and its variability across the doped block, five sub-samples of the cement-doped mixture were taken at four different stages (heights) of infilling (as described in Fig. A4), for a total of 20 dose rate control samples covering the entire cube (from edges to centre).

The final dimensions of the cubic block are 60 cm × 60 cm × 60 cm, with a horizontal 28 cm-deep cavity in its centre, constructed by inserting a 8.5 cm-diameter PVC tube (gauge: 1 mm thick) during the infilling of the cement-doped mixture. This tube serves as a cavity to accommodate cylindrical gamma spectrometer probes containing up to 3" × 3" diameter crystals (Fig. 2). The cylindrical hole does not extend all the way through the block, i.e., unlike the Oxford blocks. Additional details and pictures about the construction may be found in the Appendix.

3. Dose rate evaluation

A combination of various independent techniques has been employed to evaluate the gamma dose rate of the block, as detailed in the following sections.

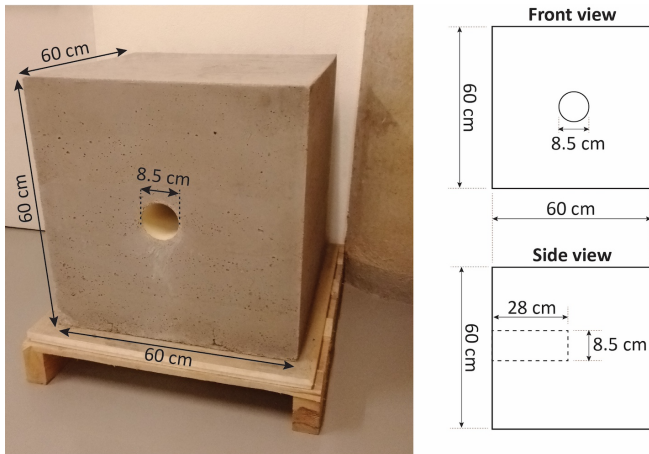


Figure 2: Picture and schematic view of the granite-doped concrete block at CENIEH, Spain.

3.1. ICP-MS/OES analysis of block sub-samples

A total of 20 samples of 15–20 g each, was collected in four successive stages during the infilling of the doped-block as described above. Consequently, each set of five samples corresponds to a given height in the cube: 12 cm (samples 1–5), 22 cm (6–10), 32 cm (11–15) and 50 cm (16–20). The wet samples were air-dried in the same conditions (i.e., in the CENIEH’s second basement) and for as long as the block (1 month). Then, each dry sample was finely powdered to $<1\ \mu\text{m}$ using a Retsch Planetary Ball Mill PM-100 to ensure homogenisation. Radioelement concentrations were obtained by Inductively Coupled Plasma (ICP) Mass Spectrometry (U and Th) and ICP Optical (Atomic) Emission Spectrometry (K), following a 4-acid digestion procedure including hydrofluoric, nitric, perchloric and hydrochloric acids in teflon tubes. Analyses were performed by Genalysis Laboratory Services at Maddington (Perth, Australia). Individual samples were also collected from the main constituents of the block (i.e., Porriño granite, cement and sand) for comparison.

3.2. $\text{Al}_2\text{O}_3:\text{C}$ dosimeters

One OSL dosimeter composed of two $\text{Al}_2\text{O}_3:\text{C}$ thin chips positioned at the end of a 30 cm-long aluminium tube was left in the central hole of the block (touching the lower side of the hole) for 289 days (~ 9.6 months). The reading of the chips was performed at the University of Bordeaux, France, following a procedure similar to Kreutzer et al. (2018). An effective gamma dose rate was obtained after (i) removing a minor cosmic dose rate contribution, which was estimated to $21 \pm 2\ \mu\text{Gy a}^{-1}$ (using Prescott & Hutton, 1994) given the location of the block in the basement of the building, two floors below ground level, and (ii) considering the gamma-ray attenuation induced by the aluminium tube that housed the OSL dosimeters (correction factor of 1.07 ± 0.01).

3.3. Portable gamma spectrometry probes

A series of 4π -measurements ($n = 46$) have been carried out in the block between 2019 and 2024 using different gamma spectrometer probes belonging to various institutions /research laboratories:

- Probe #1: $2'' \times 2''$ NaI(Tl) gamma spectrometer probe connected to a Canberra Inspector-1000 multichannel analyser (CENIEH, Spain).
- Probes #2 and #3: $2'' \times 2''$ NaI(Tl) gamma spectrometer probes connected to a Mirion-Canberra Osprey-PKG multichannel analyser (CENIEH, Spain).
- Probe #4: $2'' \times 2''$ NaI(Tl) gamma spectrometer probe connected to a Canberra Inspector-1000 multichannel analyser (Griffith University, Australia).
- Probes #5 and #6: two separate $2'' \times 2''$ NaI(Tl) gamma spectrometer probes connected to Canberra Inspector-1000 multichannel analysers (University of Adelaide, Australia).

All of these probes had been previously calibrated with the Oxford blocks (Rhodes & Schwenninger, 2007) and were used to calculate the CENIEH block gamma dose rate using either the Threshold method (probes #1–4) or Windows method (probes #5–6), following the procedures described in Duval & Arnold (2013) and Arnold et al. (2012), respectively. Additionally, the Matlab-based OxGamma program (Kumar et al., 2022) was employed in parallel for selected spectra (probes #1 to #4) to determine the block gamma dose rate via the Threshold approach, in order to evaluate any potential bias related to the specific evaluation procedure used.

4. Results and discussion

4.1. ICP-MS/OES analysis of block samples

ICP-MS/OES analytical results show significant variability in radioelement concentrations (relative standard deviations between 27 % and 44 %), with U, Th and K ranging from 3.42–7.39 ppm, 7.15–28.1 ppm and 1.11–3.59 %, respectively (Table 1). The U and K values are within the range of radioelement concentrations measured from the main individual components of the block, i.e., the pure granite, sand aggregate and cement samples. In contrast, many samples from the block show a significantly higher Th concentration (17 ppm on average) than in the reference samples, which have values of 10.5 ppm (granite) to 15 ppm (cement) (Table 1). This unexpected outcome might result from the heterogeneity of the rock, suggesting that Th-bearing minerals may be noticeably underrepresented in the single sample of the Porriño granite analysed by ICP. This may also explain why the individual sample from the cement returned higher Th concentration than the granite.

Using the dose rate conversion factors from Guérin et al. (2011) and assuming infinite matrix conditions and a water content of 0 %, a mean gamma dose rate of

Table 1: Radioelement concentrations measured by ICP-MS/OES. Uncertainties are shown at 1σ . Samples 1–10 and 11–20 were collected from mixtures A and B, respectively. Samples 1–5, 6–10, 11–15 and 16–20 correspond to different phases of infill (see further details in Appendix A4).

| Sample | Height [cm] ¹ | U [ppm] | Th [ppm] | K [%] |
|-----------------------------|--------------------------|----------------------|-----------------------|----------------------|
| LM-19276-01-1 | 12 | 6.22 ± 0.16 | 25.31 ± 1.02 | 3.42 ± 0.10 |
| LM-19276-01-2 | 12 | 6.41 ± 0.16 | 27.20 ± 1.09 | 3.52 ± 0.11 |
| LM-19276-01-3 | 12 | 7.39 ± 0.19 | 27.63 ± 1.11 | 3.46 ± 0.10 |
| LM-19276-01-4 | 12 | 5.73 ± 0.15 | 23.59 ± 0.95 | 3.49 ± 0.10 |
| LM-19276-01-5 | 12 | 5.59 ± 0.14 | 22.53 ± 0.91 | 3.59 ± 0.11 |
| LM-19276-01-6 | 22 | 6.94 ± 0.18 | 28.10 ± 1.13 | 3.17 ± 0.09 |
| LM-19276-01-7 | 22 | 5.77 ± 0.15 | 21.76 ± 0.88 | 3.30 ± 0.10 |
| LM-19276-01-8 | 22 | 5.65 ± 0.14 | 20.54 ± 0.83 | 3.05 ± 0.09 |
| LM-19276-01-9 | 22 | 6.14 ± 0.16 | 22.70 ± 0.91 | 3.29 ± 0.10 |
| LM-19276-01-10 | 22 | 6.34 ± 0.16 | 22.15 ± 0.89 | 3.09 ± 0.09 |
| LM-19276-01-11 | 32 | 4.22 ± 0.11 | 11.65 ± 0.47 | 1.75 ± 0.05 |
| LM-19276-01-12 | 32 | 3.81 ± 0.10 | 12.77 ± 0.51 | 1.57 ± 0.05 |
| LM-19276-01-13 | 32 | 3.90 ± 0.10 | 13.69 ± 0.55 | 1.67 ± 0.05 |
| LM-19276-01-14 | 32 | 3.84 ± 0.10 | 10.32 ± 0.42 | 1.73 ± 0.05 |
| LM-19276-01-15 | 32 | 4.28 ± 0.11 | 16.21 ± 0.65 | 1.64 ± 0.05 |
| LM-19276-01-16 | 50 | 3.95 ± 0.10 | 9.40 ± 0.38 | 1.19 ± 0.04 |
| LM-19276-01-17 | 50 | 3.42 ± 0.09 | 7.15 ± 0.29 | 1.12 ± 0.03 |
| LM-19276-01-17 ² | 50 | 3.46 ± 0.09 | 7.33 ± 0.30 | 1.12 ± 0.03 |
| LM-19276-01-18 | 50 | 3.85 ± 0.10 | 10.61 ± 0.43 | 1.16 ± 0.03 |
| LM-19276-01-19 | 50 | 3.53 ± 0.09 | 7.68 ± 0.31 | 1.11 ± 0.03 |
| LM-19276-01-20 | 50 | 3.44 ± 0.09 | 9.02 ± 0.36 | 1.23 ± 0.04 |
| Mean ± 1 std. dev. (%) | 12–50 | 4.95 ± 1.32 (26.7 %) | 17.02 ± 7.48 (44.0 %) | 2.32 ± 1.02 (44.1 %) |
| Min | 12–50 | 3.42 ± 0.09 | 7.15 ± 0.29 | 1.11 ± 0.03 |
| Max | 12–50 | 7.39 ± 0.19 | 28.10 ± 1.13 | 3.59 ± 0.11 |
| Mean ± 1 std. dev. (%) | 12 | 3.49 ± 0.07 (1.9 %) | 25.25 ± 2.21 (8.8 %) | 6.27 ± 0.71 (11.4 %) |
| Mean ± 1 std. dev. (%) | 22 | 3.18 ± 0.11 (3.6 %) | 23.05 ± 2.93 (12.7 %) | 6.17 ± 0.51 (8.3 %) |
| Mean ± 1 std. dev. (%) | 32 | 1.67 ± 0.07 (4.2 %) | 12.93 ± 2.23 (17.2 %) | 4.01 ± 0.22 (5.5 %) |
| Mean ± 1 std. dev. (%) | 50 | 1.15 ± 0.05 (4.4 %) | 8.36 ± 1.46 (17.4 %) | 3.54 ± 0.18 (5.0 %) |
| Main constituents | | | | |
| Porriño granite | | 11.63 ± 0.30 | 10.52 ± 0.30 | 2.83 ± 0.08 |
| Sandy aggregate | | 2.46 ± 0.06 | 2.15 ± 0.06 | 0.30 ± 0.01 |
| Cement | | 1.72 ± 0.04 | 15.09 ± 0.04 | 2.72 ± 0.08 |

¹ Height corresponds to the approximated vertical distance (in cm) from the bottom of the cube.

² Note that two sub-samples of sample 17 were collected. The two subsamples return similar radioelement concentrations (within error).

$1926 \pm 463 \mu\text{Gy a}^{-1}$ may be tentatively calculated for the whole block from the mean radioelement concentrations (Table 1). This value should however be treated with extreme caution, as it is unlikely to provide a reliable estimate of the true gamma dose rate given the significant variability observed between the 20 sub-samples from the block (Table 1). We presently suspect that this variability may mostly be due to the relative inhomogeneity in the mixing of the various components of the block (see also [Bowman, 1976](#); [Murray, 1981](#), for further information on that specific matter), resulting in the spatial heterogeneity of radioelement distribution. Interestingly, this hypothesis is supported by the ICP results from each set of samples collected at increasing height in the block: they show a significant vertical gradient in radioele-

ment concentrations, with lower values towards the top of the block (U: 3.5 ppm to 1.2 ppm; Th: 25.3 ppm to 8.4 ppm; K: 6.3 % to 3.5 %; Table 1). Moreover, within a given set of samples (i.e., corresponding to a given height), radioelement concentrations also show a non-negligible variability (1 relative standard deviation) of 1.9–4.4 %, 8.8–17.4 % and 5.0–11.4 % for U, Th and K, respectively (Table 1). Consequently, the block shows an overall (vertical and horizontal) inhomogeneity. Despite our best efforts to ensure a relative homogeneous mixing, empirical data indicate that this was not achieved (see also how the two mixtures A and B compare in terms of radioelement concentrations, i.e., samples 1–10 vs. 11–20 in Table 1). We do acknowledge that our precautions were probably not as thorough as those em-

ployed for the construction of the Oxford Blocks (Bowman, 1976; Murray et al., 1978; Murray, 1981), and we would welcome any feedback, perhaps resulting from similar experiences, from the LED community on this matter.

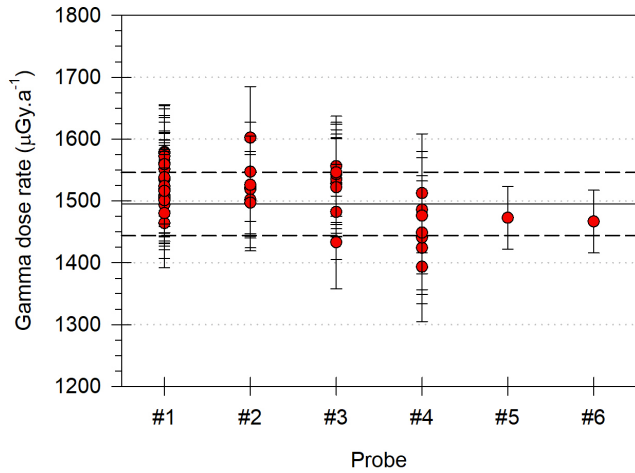


Figure 3: Graphical overview of the gamma dose rate measured for the granite-doped block with NaI(Tl) probes #1 to #6. Numerical values may be found in Table 2. The horizontal solid and short dash lines represent the value and associated 1σ uncertainties obtained from the $\text{Al}_2\text{O}_3:\text{C}$ dosimeters ($1495 \pm 51 \mu\text{Gy a}^{-1}$).

Table 2 (next page): Overview of the granite block gamma dose rate values measured over a five-year period with various NaI(Tl) gamma spectrometer probes. Gamma dose rate values have been calculated with the Threshold method following two different procedures: (i) Arnold et al. (2012) and Duval & Arnold (2013), and (ii) OxGamma (Kumar et al., 2022). The gamma dose rate ratios (FGS/dosimeter) were obtained by comparing the field gamma spectrometer (FGS) dose rates with the independent values obtained using the $\text{Al}_2\text{O}_3:\text{C}$ dosimeters ($1495 \pm 51 \mu\text{Gy a}^{-1}$). Note that a minor internal gamma dose rate contribution from the NaI(Tl) probe itself ($\sim 10 \mu\text{Gy a}^{-1}$, corresponding to $<0.1\%$ of the measured gamma dose rate) was subtracted from all values derived using the procedure of Duval & Arnold (2013), unlike for the OxGamma results. Uncertainties are shown at 1σ . Key: n.c. = not calculated.

4.2. $\text{Al}_2\text{O}_3:\text{C}$ dosimeters

A mean effective gamma dose rate of $1495 \pm 51 \mu\text{Gy a}^{-1}$ was obtained from the two $\text{Al}_2\text{O}_3:\text{C}$ chips. The relative associated error (3.4%) includes the calibration source error (2.9%), and its magnitude illustrates the limited dose variability among the chips, which returned consistent values differing by $<2\%$.

4.3. Portable gamma spectrometry

All measurements made using the six different gamma spectrometer probes return consistent values (within $\pm 2.8\%$ on average), regardless of the probe employed (Tables 2–3; Fig. 3). A mean Threshold-based gamma dose rate of $1514 \pm 43 \mu\text{Gy a}^{-1}$ (1 s.d.) can be calculated from all measurements ($n = 44$) made with probes #1 to #4. Each probe shows relatively high measurement repeatability, with a relative standard deviation of $<4\%$ in the gamma dose rate values (probe #1 = 2.0% [$n = 20$]; probe #2 = 2.3% [$n = 7$]; probe #3 = 2.5% [$n = 9$]; probe #4: 2.7% [$n = 8$]). These values likely reflect the inherent precision of the gamma spectrometers used in this study, and are consistent with the reproducibility uncertainty (2.1%) previously estimated by Arnold et al. (2012) for a similar gamma spectrometer. The mean Threshold-based gamma dose rate values obtained for each probe are in close agreement at 1σ : $1527 \pm 31 \mu\text{Gy a}^{-1}$ (#1), $1531 \pm 35 \mu\text{Gy a}^{-1}$ (#2), $1519 \pm 38 \mu\text{Gy a}^{-1}$ (#3), $1459 \pm 39 \mu\text{Gy a}^{-1}$ (#4). The slightly lower mean value obtained for probe #4 is especially impacted by a single low outlying measurement (2308GU, Table 2), given the small size of the data set ($n = 8$). An average gamma dose rate of $1468 \pm 31 \mu\text{Gy a}^{-1}$ may be calculated instead for this probe when excluding this measurement (Table 2), which is in closer agreement with the results obtained from the other probes.

The Threshold-based gamma dose rates obtained using OxGamma are consistent with (i.e., within error of) those calculated using the procedures described in Duval & Arnold (2013) for all probe measurements. The corresponding results differ by 1–4% on average for a given probe (Table 2), by about 1.5% when considering all measurements ($n = 44$), and the individual deviation observed for each spectrum is consistently $<5\%$ (with three exceptions). The differences observed partly originate from the subtraction of the gamma dose rate contribution from the NaI(Tl) probe itself ($\sim 10 \mu\text{Gy a}^{-1}$, corresponding to $<0.1\%$ of the measured gamma dose rate), which is not considered by OxGamma, unlike Duval & Arnold (2013). When including this component in both evaluation procedures, the relative difference drops from 1.5% to $<1\%$ on average when considering all measurements (Table 2). Finally, it can be observed from Table 2 that OxGamma offers an overall higher measurement repeatability, with gamma dose rate values showing slightly lower variability, and hence higher consistency, for a given probe (probe #1 = 1.3 vs. 2.0% [$n = 20$]; probe #2 = 0.8 vs. 2.3% [$n = 7$]; probe #3 =

| Date | Probe | Spectrum ID | Duval and Arnold (2013) | | OxGamma | |
|----------------------------|-------|-------------|-------------------------------------------|---------------------------------------|-------------------------------------------|---------------------------------------|
| | | | Gamma dose rate [$\mu\text{Gy a}^{-1}$] | Gamma dose rate ratio (FGS/dosimeter) | Gamma dose rate [$\mu\text{Gy a}^{-1}$] | Gamma dose rate ratio (FGS/dosimeter) |
| Nov-19 | #1 | 1965N | 1 505 \pm 74 | 1.01 | 1 567 \pm 78 | 1.05 |
| Dec-19 | #1 | 1972N | 1 519 \pm 75 | 1.02 | 1 563 \pm 78 | 1.05 |
| Feb-20 | #1 | 2010N | 1 579 \pm 77 | 1.06 | 1 566 \pm 78 | 1.05 |
| Mar-20 | #1 | 2012N | 1 561 \pm 77 | 1.04 | 1 566 \pm 78 | 1.05 |
| May-20 | #1 | 2013N | 1 494 \pm 73 | 1.00 | 1 557 \pm 78 | 1.04 |
| Jun-20 | #1 | 2017N | 1 534 \pm 75 | 1.03 | 1 559 \pm 78 | 1.04 |
| Jul-20 | #1 | 2019N | 1 551 \pm 76 | 1.04 | 1 577 \pm 79 | 1.05 |
| Aug-20 | #1 | 2021N | 1 577 \pm 77 | 1.05 | 1 562 \pm 78 | 1.04 |
| Sep-20 | #1 | 2023N | 1 572 \pm 77 | 1.05 | 1 577 \pm 79 | 1.06 |
| Oct-20 | #1 | 2025N | 1 536 \pm 75 | 1.03 | 1 542 \pm 77 | 1.03 |
| Nov-20 | #1 | 2027N | 1 509 \pm 74 | 1.01 | 1 534 \pm 77 | 1.03 |
| Dec-20 | #1 | 2028N | 1 464 \pm 72 | 0.98 | 1 526 \pm 76 | 1.02 |
| Jan-21 | #1 | 2102N | 1 523 \pm 75 | 1.02 | 1 528 \pm 76 | 1.02 |
| Feb-21 | #1 | 2104N | 1 559 \pm 76 | 1.04 | 1 524 \pm 76 | 1.02 |
| Mar-21 | #1 | 2105N | 1 538 \pm 75 | 1.03 | 1 524 \pm 76 | 1.02 |
| Apr-21 | #1 | 2111N | 1 506 \pm 74 | 1.01 | 1 544 \pm 77 | 1.03 |
| May-21 | #1 | 2118N | 1 524 \pm 75 | 1.02 | 1 529 \pm 76 | 1.02 |
| Aug-21 | #1 | 2123N | 1 501 \pm 74 | 1.00 | 1 526 \pm 76 | 1.02 |
| Oct-21 | #1 | 2132N | 1 516 \pm 74 | 1.01 | 1 522 \pm 76 | 1.02 |
| Nov-21 | #1 | 2169N | 1 480 \pm 73 | 0.98 | 1 546 \pm 77 | 1.03 |
| Oct-22 | #2 | 2212A | 1 522 \pm 79 | 1.02 | 1 519 \pm 76 | 1.02 |
| Jun-23 | #2 | 2322A | 1 519 \pm 79 | 1.02 | 1 518 \pm 76 | 1.02 |
| Aug-23 | #2 | 2326A | 1 502 \pm 78 | 1.00 | 1 517 \pm 76 | 1.01 |
| Aug-23 | #2 | 2325A | 1 497 \pm 78 | 1.00 | 1 531 \pm 77 | 1.02 |
| Feb-24 | #2 | 2413A | 1 547 \pm 80 | 1.03 | 1 545 \pm 77 | 1.03 |
| Jun-24 | #2 | 2439A | 1 602 \pm 83 | 1.07 | 1 510 \pm 76 | 1.01 |
| Aug-24 | #2 | 2449A | 1 526 \pm 79 | 1.02 | 1 524 \pm 76 | 1.02 |
| Sep-22 | #3 | 2211B | 1 556 \pm 81 | 1.04 | 1 531 \pm 77 | 1.02 |
| Oct-22 | #3 | 2212B | 1 528 \pm 80 | 1.02 | 1 525 \pm 76 | 1.02 |
| Jun-23 | #3 | 2311B | 1 535 \pm 80 | 1.03 | 1 562 \pm 78 | 1.04 |
| Aug-23 | #3 | 2314B | 1 543 \pm 81 | 1.03 | 1 540 \pm 77 | 1.03 |
| Aug-23 | #3 | 2313B | 1 482 \pm 77 | 0.99 | 1 541 \pm 77 | 1.03 |
| Aug-23 | #3 | 2315B | 1 522 \pm 79 | 1.02 | 1 539 \pm 77 | 1.03 |
| Feb-24 | #3 | 2401B | 1 522 \pm 80 | 1.02 | 1 541 \pm 77 | 1.03 |
| Jun-24 | #3 | 2408B | 1 546 \pm 81 | 1.03 | 1 521 \pm 76 | 1.02 |
| Aug-24 | #3 | 2417B | 1 433 \pm 75 | 0.96 | 1 536 \pm 77 | 1.03 |
| Sep-21 | #4 | 2115GU | 1 486 \pm 94 | 0.99 | 1 520 \pm 76 | 1.01 |
| Oct-21 | #4 | 2120GU | 1 424 \pm 90 | 0.95 | 1 510 \pm 76 | 1.00 |
| Jul-22 | #4 | 2224GU | 1 441 \pm 92 | 0.96 | 1 520 \pm 76 | 1.01 |
| Jul-22 | #4 | 2225GU | 1 449 \pm 92 | 0.97 | 1 514 \pm 76 | 1.00 |
| Aug-23 | #4 | 2308GU | 1 393 \pm 89 | 0.93 | 1 518 \pm 76 | 1.00 |
| Jul-24 | #4 | 2401GU | 1 512 \pm 96 | 1.01 | 1 518 \pm 77 | 1.00 |
| Jul-24 | #4 | 2402GU | 1 476 \pm 94 | 0.99 | 1 521 \pm 76 | 1.01 |
| Sep-24 | #4 | 2409GU | 1 488 \pm 95 | 1.00 | 1 511 \pm 76 | 1.00 |
| Mean \pm 1 std. dev. (%) | | | | | | |
| | #1 | | 1 527 \pm 31 (2.0 %) | 1.02 | 1 547 \pm 20 (1.3 %) | 1.03 |
| | #2 | | 1 531 \pm 35 (2.3 %) | 1.02 | 1 523 \pm 11 (0.8 %) | 1.02 |
| | #3 | | 1 519 \pm 38 (2.5 %) | 1.02 | 1 537 \pm 12 (0.8 %) | 1.03 |
| | #4 | | 1 459 \pm 39 (2.7 %) | 0.98 | 1 517 \pm 4 (0.3 %) | 1.01 |
| | All | | 1 514 \pm 43 (2.9 %) | 1.02 | 1 537 \pm 19 (1.2 %) | 1.03 |
| | | | [1 524 \pm 43] ¹ | | | |

¹ Average value including the minor internal component from the probe ($10 \mu\text{Gy a}^{-1}$), to facilitate a direct comparison with the corresponding OxGamma result.

Table 3: Radioelement concentrations measured by field gamma spectrometry using the Windows method outlined in Arnold et al. (2012). Gamma dose rates have been calculated using the dose rate conversion factors of Guérin et al. (2011) and a water content of 0%. No internal gamma dose rate contribution from the NaI(Tl) probe itself was considered here. The gamma dose rate ratios (FGS/dosimeter) were obtained by comparing the field gamma spectrometer (FGS) dose rates with the independent values obtained using the Al₂O₃:C dosimeters ($1\,495 \pm 51 \mu\text{Gy a}^{-1}$). Elemental concentration uncertainties and gamma dose rate uncertainties are shown at 1σ .

| Date | Probe | Spectrum | U [ppm] | Th [ppm] | K [%] | Gamma dose rate [$\mu\text{Gy a}^{-1}$] | Gamma dose rate ratio (FGS/dosimeter) |
|--------|-------|----------|-----------------|------------------|-----------------|-------------------------------------------|---------------------------------------|
| Jul-22 | #5 | 2275a | 4.30 ± 0.28 | 12.71 ± 0.73 | 1.56 ± 0.08 | $1\,473 \pm 51$ | 0.99 |
| Jul-24 | #6 | 2420c | 4.23 ± 0.28 | 12.53 ± 0.72 | 1.61 ± 0.09 | $1\,467 \pm 51$ | 0.98 |

0.8 vs. 2.5% [$n = 9$]; probe #4: = 0.3 vs. 2.7% [$n = 8$]). In summary, these results provide confidence that the two independent evaluation procedures are directly comparable and the resultant gamma dose rates are reproducible.

The gamma dose rate values calculated using the Windows method (Arnold et al., 2012) for probes #5 and #6 ($1\,473 \pm 51 \mu\text{Gy a}^{-1}$ and $1\,467 \pm 51 \mu\text{Gy a}^{-1}$, respectively; Table 3) are not only consistent with each other (differing by $<1\%$), but are also in agreement at 1σ with the various Threshold-based gamma dose rate values obtained for probes #1 to #4 obtained with either Duval & Arnold (2013)'s procedure or OxGamma (Table 2). Moreover, the following average radioelement concentrations and associated errors may be calculated from these two independent measurements: $K = 1.58 \pm 0.08\%$, $U = 4.26 \pm 0.28 \text{ ppm}$, $Th = 12.62 \pm 0.72 \text{ ppm}$. Unlike the average radioelement concentrations derived from ICP analyses of block sub-samples (section 4.1), these results may be regarded as reliable spatially averaged estimates of the bulk radioelement concentrations when performing dosimetry evaluations in the central hole of the block. To sum up, independent dosimetry assessments made using different gamma probes and data evaluation procedures (Threshold vs. Windows; Duval & Arnold (2013) vs. OxGamma) return consistent results and support the robustness of the combined data set.

4.4. Comparison of dosimetry approaches

A comparison of the various gamma dose rate values obtained independently or semi-independently using different dosimetry evaluations provides useful insights into their accuracy. In this context, the mean Threshold-based gamma dose rate of $1\,514 \pm 43 \mu\text{Gy a}^{-1}$ (1 s.d.) calculated from all measurements (Duval & Arnold (2013)'s evaluation procedure) made with probes #1 to #4 is in excellent agreement with the independent gamma dose rate ($1\,495 \pm 51 \mu\text{Gy a}^{-1}$) obtained from the Al₂O₃:C dosimeter (deviation $\sim 2\%$). Additionally, the deviation observed for each spectrum does not exceed 5% of the Al₂O₃:C dosimeter gamma dose rate in most cases (with a few exceptions ($n = 3$); Table 2), and it is consistently $<10\%$ for all spectra, demonstrating sufficient reproducibility for both techniques (Fig. 3).

The two Windows-based gamma dose rate values of

$1\,473 \pm 51 \mu\text{Gy a}^{-1}$ (probe #5) and $1\,467 \pm 51 \mu\text{Gy a}^{-1}$ (probe #6) are also consistent at 1σ with the Al₂O₃:C gamma dose rate estimate ($1\,495 \pm 51 \mu\text{Gy a}^{-1}$, with the two datasets differing by only $\sim 2\%$). To sum up, all in situ gamma dose rate results obtained using NaI probe gamma spectrometry and Al₂O₃:C dosimeters are within close range of each other. Finally, it is noteworthy that both the NaI gamma probes and the Al₂O₃:C dosimeters produce gamma dose rates that are significantly lower (by $>400 \mu\text{Gy a}^{-1}$) than that initially estimated from all the ICP analyses; though the two sets of results actually overlap at 1σ given the large uncertainty associated with the ICP measurements. This confirms that the latter should not be regarded as a reliable estimate of the true gamma dose rate of the block at the central hole measurement position, mostly owing to spatial heterogeneity in the granite-doped concrete block mixture, although we cannot discard that other sources of uncertainty may also be possibly involved (see discussion in Bowman, 1976; Murray, 1981).

5. Conclusion

We present a new dosimetry reference block that complements a range of similar structures available at various luminescence and ESR dating laboratories around the world. Despite apparent non-negligible heterogeneity in the spatial distribution of radioelements in the block as suggested by the significant variability of the ICP analytical results from 20 strategically-collected samples, the gamma dose rates measured in the central hole position with two independent techniques (Al₂O₃:C dosimeters and NaI probe gamma spectrometry) and using various evaluation procedures are all within close range of each other. The consistency of these results suggests that the true gamma dose rate at the centre of the block has been properly constrained, although efforts are ongoing to further refine this initial evaluation through a combination of experimental and modeling procedures. Based on the experience acquired through decades of investigations around the Oxford Blocks (e.g., Bowman, 1976; Murray et al., 1978; Murray, 1981; Rhodes & Schwenninger, 2007, and references therein), we also acknowledge that several aspects of the CENIEH block will deserve further attention (e.g., density, disequilibrium, water content, spatial heterogeneity) in order to ensure its exhaustive characteriza-

tion. In this regard, we welcome future collaborative initiatives or any scientific inputs on this matter. The CENIEH reference block is made available to all members of the trapped charge dating community for instrument calibration and reproducibility assessments, including intercomparison studies with similar dosimetry reference materials at other laboratories.

Acknowledgements

We thank Carlos Pérez Garrido, CENIEH, for his contribution to the gamma dose rate evaluation from field gamma spectra, as well as David Martínez Asturias, Carlos Sáiz Domínguez, Jaime Torres, CENIEH, and Adolfo Alonso and his team "Construcciones A10" for their invaluable help with the construction of the block. A major thank you to "Construcciones Ortega S.A.", the Burgos company commissioned by the Burgos City Council to renovate the pavement of its emblematic Plaza Mayor, for kindly donating the slabs of the pink Porriño granite to G. I. L., without which this block could not have been made. Raju Kumar acknowledges support from UK Research and Innovation (Natural Environment Research Council grant reference NE/T001313/1). This research benefitted from the scientific framework given by the University of Bordeaux's IdEx "Investments for the Future" program / GPR "Human Past". We would also like to extend our thanks to the reviewer and editor for their constructive comments on the manuscript.

References

- Arnold, L. J., Duval, M., Falguères, C., Bahain, J.-J., and Demuro, M. *Portable gamma spectrometry with cerium-doped lanthanum bromide scintillators: Suitability assessments for luminescence and electron spin resonance dating applications*. *Radiation Measurements*, 47(1): 6–18, 2012.
- Bowman, S. *Thermoluminescent Dating: The Evaluation of Radiation Dosage (Appendix A.5. Environmental Dosimetry)*. PhD thesis, University of Oxford, 1976.
- Duval, M. and Arnold, L. J. *Field gamma dose-rate assessment in natural sedimentary contexts using LaBr₃ (Ce) and NaI (Tl) probes: A comparison between the "threshold" and "windows" techniques*. *Applied Radiation and Isotopes*, 74: 36–45, 2013.
- Gonzalez Menéndez, L., Gallastegui Suárez, G., Cuesta Fernández, A., Montero, P., Rubio Ordóñez, A., Molina, J., and Bea Barredo, F. *Petrology and geochronology of the Porriño late-Variscan pluton from NW Iberia. A model for post-tectonic plutons in collisional settings*. *Geologica Acta*, 15(4): 283–304, 2017.
- Grasty, R. L. and Minty, B. R. S. *A Guide to the Technical Specifications for Airborne Gamma-ray Surveys*. Citeseer, 1990. ISBN 0642223661.
- Grossi, C. M., Alonso, F. J., Esbert, R. M., and Rojo, A. *Effect of laser cleaning on granite color*. *Color Research & Application*, 32(2): 152–159, 2007.
- Guérin, G., Mercier, N., and Adamiec, G. *Dose-rate conversion factors: update*. *Ancient TL*, 29: 5–8, 2011.
- Kreutzer, S., Martin, L., Guérin, G., Tribolo, C., Selva, P., and Mercier, N. *Environmental dose rate determination using a passive dosimeter: Techniques and workflow for α -Al₂O₃:C chips*. *Geochronometria*, 45(1): 56–67, 2018.
- Kumar, R., Frouin, M., Gazack, J., and Schwenninger, J.-L. *OxGamma: A MATLAB based application for the analysis of gamma-ray spectra*. *Radiation Measurements*, 154: 106761, 2022.
- Martin, L. *Caractérisation et modélisation d'objets archéologiques en vue de leur datation par des méthodes paléo-dosimétriques: simulation des paramètres dosimétriques sous Geant4*. PhD thesis, Université Michel de Montaigne - Bordeaux III, 2015.
- Mercier, N. and Falguères, C. *Field gamma dose-rate measurement with a NaI(Tl) detector: Re-evaluation of the "threshold" technique*. *Ancient TL*, 25: 1–4, 2007.
- Miallier, D., Guérin, G., Mercier, N., Pilleyre, T., and Sanzelle, S. *The Clermont radiometric reference rocks: A convenient tool for dosimetric purposes*. *Ancient TL*, 27: 37–43, 2009.
- Murray, A. *Environmental radioactivity studies relevant to thermoluminescence dating*. PhD thesis, University of Oxford, 1981.
- Murray, A., Bowman, S., and Aitken, M. *Evaluation of the gamma dose-rate contribution*. *Journal of the European Study Group on Physical, Chemical and Mathematical Techniques Applied to Archaeology (PACT)*, 2: 84–96, 1978.
- Porat, N. and Halicz, L. *Calibrating the luminescence dating laboratory*. *Geological Survey of Israel Current Research*, 10: 111–116, 1996.
- Prescott, J. R. and Hutton, J. T. *Cosmic ray contributions to dose rates for luminescence and ESR dating: large depths and long-term time variations*. *Radiation Measurements*, 23(2–3): 497–500, 1994.
- Rhodes, E. and Schwenninger, J.-L. *Dose rates and radioisotope concentrations in the concrete calibration blocks at Oxford*. *Ancient TL*, 25: 5–8, 2007.
- Richter, D., Dombrowski, H., Neumaier, S., Guibert, P., and Zink, A. C. *Environmental gamma dosimetry with OSL of α -Al₂O₃:C for in situ sediment measurements*. *Radiation Protection Dosimetry*, 141(1): 27–35, 2010.
- Stokes, S. *Optical dating of selected Late Quaternary aeolian sediments from the Southwestern United States*. PhD thesis, University of Oxford, 1994.

Reviewer

Ed Rhodes

Reviewer comment

The doped concrete block described in this paper represents a highly valuable addition to the calibration toolset for luminescence dating laboratories. Portable gamma spectrometry offers many benefits, with only relatively minor difficulty, but reliable calibration is important. I feel that having a secure value for the total gamma dose rate, often determined by the threshold method typically with relatively high precision, or using the window approach that provides a determination of the apparent concentrations of U, Th and K, is key to good calibration. This block delivers this with a convincing set of determinations using both $Al_2O_3:C$ chips and a suite of six pre-calibrated NaI probes measured with four different portable gamma spectrometers, displaying a high degree of internal consistency. The apparent discrepancy between the direct gamma dose rate measurements described above and ICP determinations of U, Th and K content from 20 subsamples collected during manufacture illustrate how hard it is to achieve homogeneity with real world materials. The authors note some similarity in this discrepancy with similar observations made during the construction of the Oxford blocks during the 1970s.

Appendix



Figure A1: Pink Porriño granite slabs upon arrival at the CE-NIEH, as donated to G. I. L. by Burgos' Municipality (October 31, 2018).

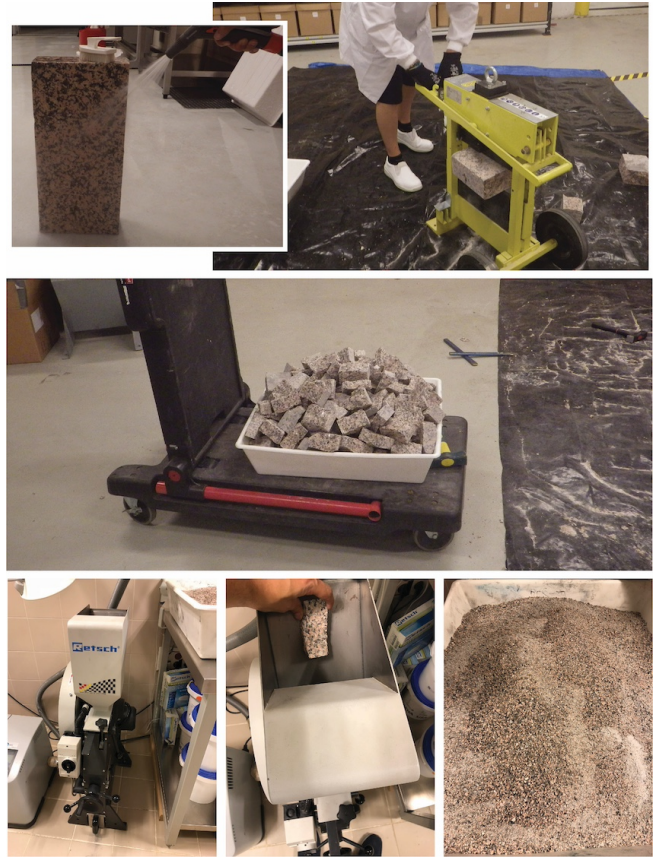


Figure A2: Slicing and crushing the Porriño granite slabs. Each slab was thoroughly cleaned of any external dirt. A guillotine-type hydraulic cutting machine was used to slice each slab into hand-sized pieces, manageable enough to crush using a laboratory jaw crusher. Care was taken to avoid cross-contamination from the ground and surroundings during slicing (a clean black tarp was spread out to contain the sliced slabs).



Figure A3: Construction of the Porriño granite-doped block (October 22, 2019). Once filled with the mixture, the plywood formwork was reinforced with strongly attached thick wooden boards to hold it together while the concrete block air-dried. It took the mixture almost 1 month to completely dry.

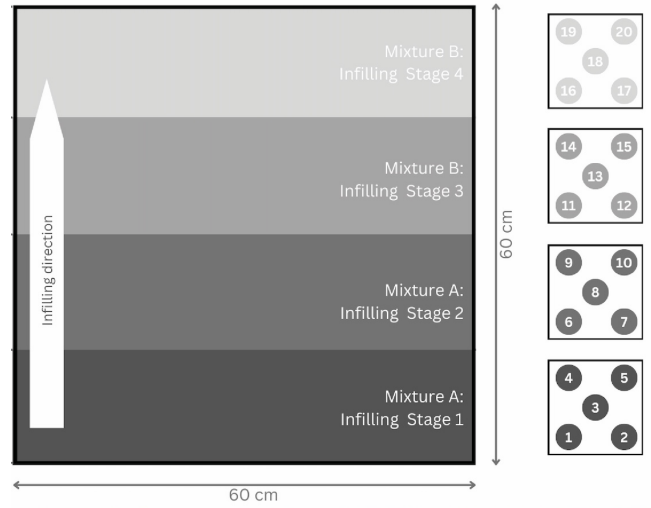


Figure A4: Sampling of the Porriño granite-doped block. Five sub-samples were taken from all four corners and centre of the formwork as it was being infilled with the mixture (two mixtures A and B poured in a total of four successive phases), for a total of 20 dose rate control samples. The sub-sampling intervals were at 12 cm from the bottom of the formwork; 22 cm of infilling (corresponding to the base of the horizontal PVC tube inserted to maintain a 8.5 cm-diameter \times 28 cm-long cavity at the centre of the doped cube); 32 cm of infilling; and at 50 cm of infilling, just 10 cm below the top of the cube.